

Supporting Information

**Engineering tri-channel orthogonal luminescence in a single nanoparticle for
Information Encryption**

Jianhao Zheng^{ab}, Pengye Du^{ab}, Ran An^{*a}, Yuan Liang^a, Yi Wei^a, Shuyu Liu^{ab},
Pengpeng Lei^{*a}, Hongjie Zhang^{*abc}

^a*State Key Laboratory of Rare Earth Resource Utilization, Changchun Institute of Applied Chemistry, Chinese Academy of Sciences, Jilin Changchun 130022, China.*

E-mail: anran@ciac.ac.cn; leipp@ciac.ac.cn; hongjie@ciac.ac.cn

^b*School of Applied Chemistry and Engineering, University of Science and Technology of China, Anhui Hefei 230026, China*

^c*Department of Chemistry, Tsinghua University, Beijing 100084, China*

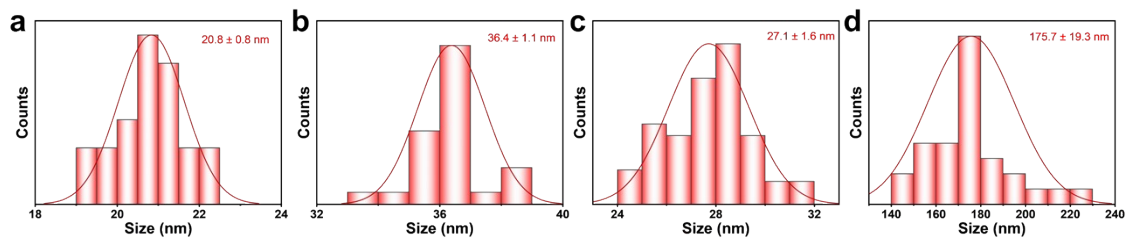


Figure S1. The corresponding size distributions of a) NaErF_4 , b and c) $\text{NaErF}_4@\text{NaYF}_4:\text{Eu}^{3+}$, and d) $\text{NaErF}_4@\text{NaYF}_4:\text{Eu}^{3+}@(\text{NaBiF}_4:\text{Yb}^{3+},\text{Tm}^{3+})$ nanoparticles.

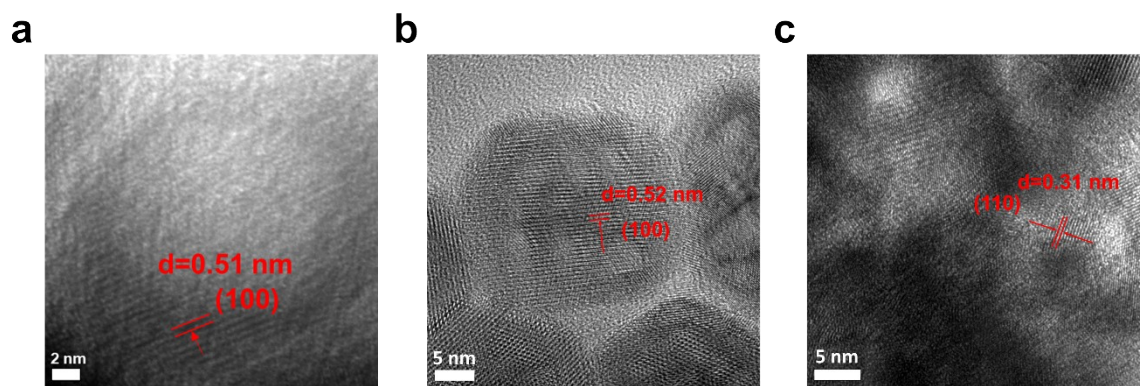


Figure S2. The high-resolution transmission electron microscopy images of the a) NaErF_4 , b) $\text{NaErF}_4@\text{NaYF}_4:\text{Eu}^{3+}$, and c) $\text{NaErF}_4@\text{NaYF}_4:\text{Eu}^{3+}@\text{NaBiF}_4:\text{Yb}^{3+},\text{Tm}^{3+}$ nanoparticles.

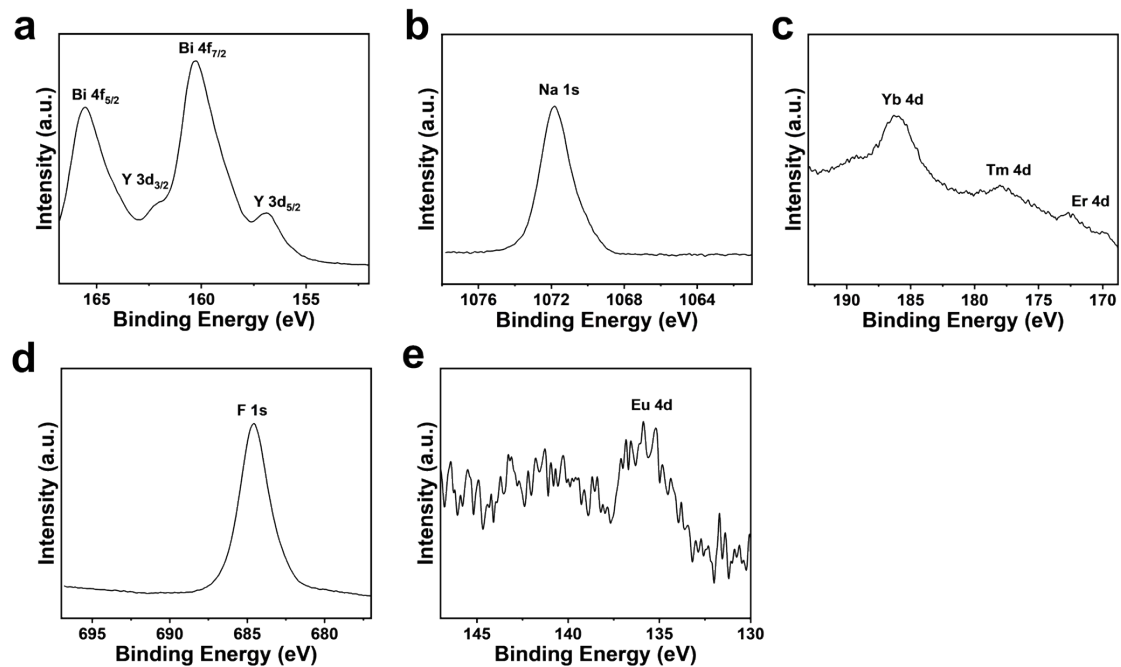


Figure S3. High-resolution X-ray photoelectron spectroscopy, a) Bi 4f and Y 3d, b) Na 1s, c) Yb 4d, Tm 4d, and Er 4d, d) F 1s, and e) Eu 4d.

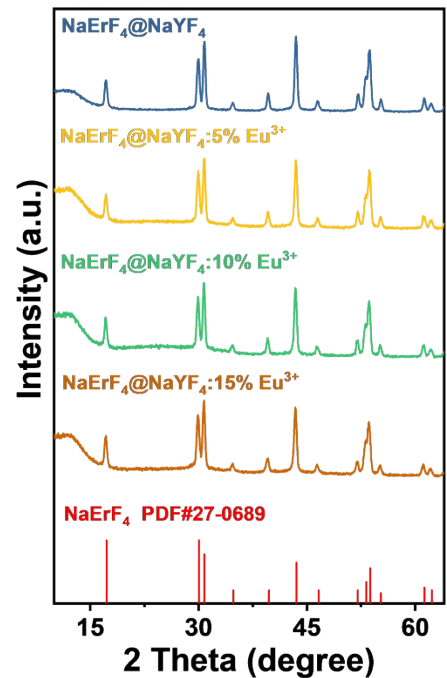


Figure S4. X-ray diffraction patterns of NaErF₄@NaYF₄:X% Eu³⁺ nanoparticles. (X = 0, 5, 10, and 15).

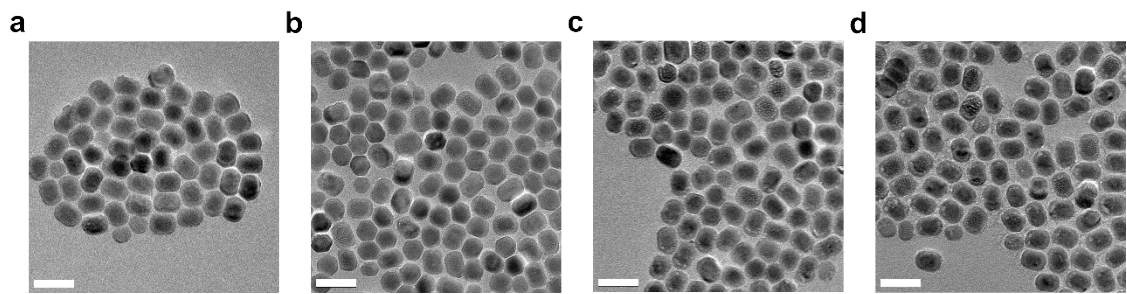


Figure S5. TEM images of the a) $\text{NaErF}_4@\text{NaYF}_4:0\%$ Eu^{3+} , b) $\text{NaErF}_4@\text{NaYF}_4:5\%$ Eu^{3+} , c) $\text{NaErF}_4@\text{NaYF}_4:10\%$ Eu^{3+} , and d) $\text{NaErF}_4@\text{NaYF}_4:15\%$ Eu^{3+} nanoparticles. (scale bar is 50 nm).

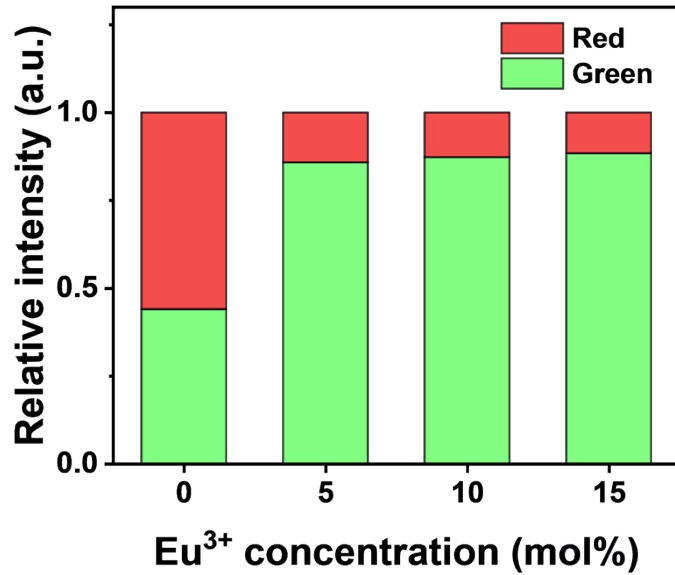


Figure S6. The relative intensity ratio of the green emission ($^2\text{H}_{11/2}, {}^4\text{S}_{3/2} \rightarrow {}^4\text{I}_{15/2}$) and the red emission (${}^4\text{F}_{9/2} \rightarrow {}^4\text{I}_{15/2}$) of the $\text{NaErF}_4@\text{NaYF}_4:\text{X}\%$ Eu³⁺ nanoparticles under 808 nm excitation. (X = 0, 5, 10, and 15).

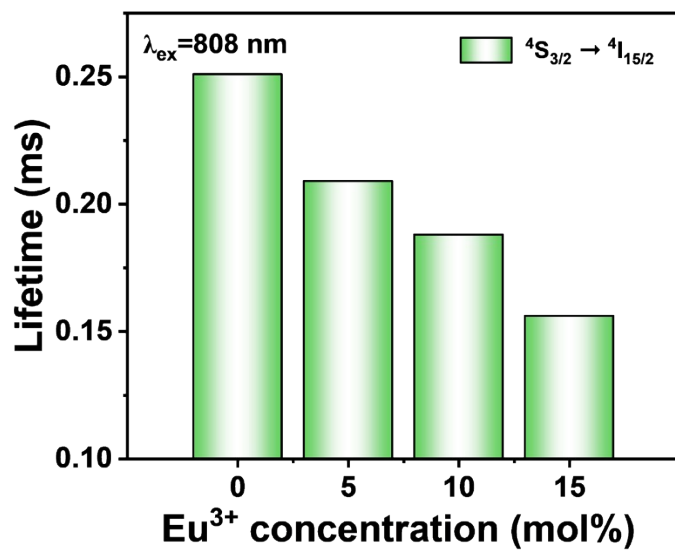


Figure S7. The lifetimes of the ${}^4S_{3/2} \rightarrow {}^4I_{15/2}$ transition of $\text{NaErF}_4 @ \text{NaYF}_4 : \text{X}\% \text{ Eu}^{3+}$ nanoparticles under 808 nm excitation. ($\text{X} = 0, 5, 10$, and 15).

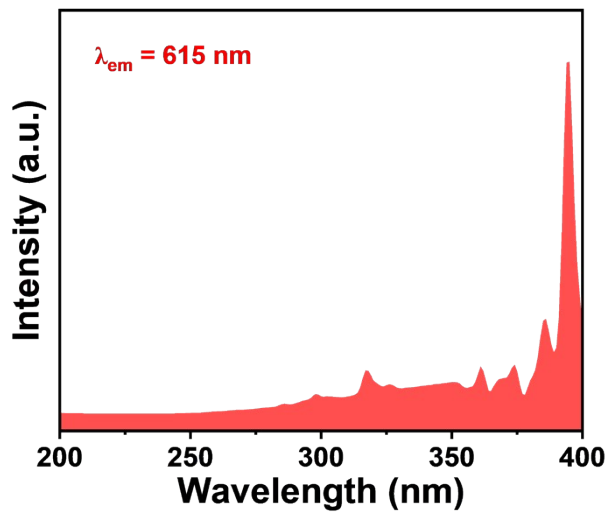


Figure S8. The excitation spectrum of the $\text{NaErF}_4@\text{NaYF}_4:\text{Eu}^{3+}$ nanoparticles.

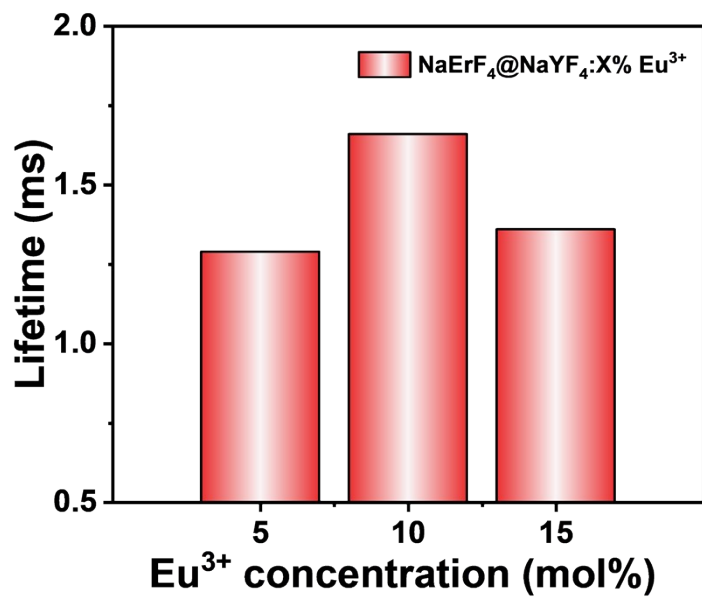


Figure S9. The lifetimes of the $^5D_0 \rightarrow ^7F_2$ transition of $\text{NaErF}_4@\text{NaYF}_4:\text{X}\%$ Eu^{3+} nanoparticles. ($\text{X} = 5, 10$, and 15).

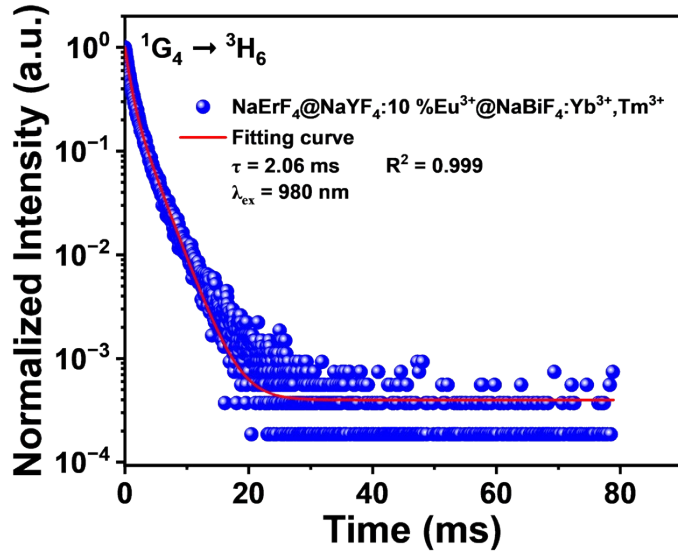


Figure S10. The time-resolved photoluminescence (TRPL) decay curves and the corresponding fitting curve of the NaErF₄@NaYF₄:10% Eu³⁺@NaBiF₄:Yb³⁺,Tm³⁺ samples under 980 nm excitation.

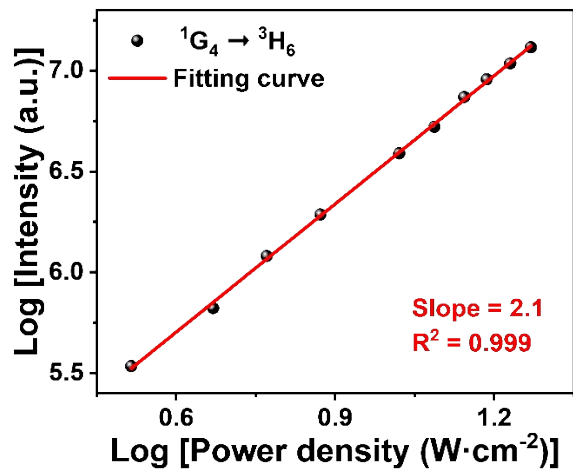


Figure S11. Pump power dependence of the ${}^1\text{G}_4 \rightarrow {}^3\text{H}_6$ transitions under 980 nm excitation.



Figure S12. Demonstration the double-color emissions of the construction of four 8-shaped pattern using $\text{NaErF}_4@\text{NaYF}_4:\text{Eu}^{3+}$ nanoparticles and $\text{NaErF}_4@\text{NaYF}_4:\text{Eu}^{3+}@\text{NaBiF}_4:\text{Yb}^{3+},\text{Tm}^{3+}$ nanoparticles. (i): $\text{NaErF}_4@\text{NaYF}_4:10\%$ Eu^{3+} and $\text{NaErF}_4@\text{NaYF}_4:10\%$ $\text{Eu}^{3+}@\text{NaBiF}_4:\text{Yb}^{3+},\text{Tm}^{3+}$ nanoparticles. (ii): $\text{NaErF}_4@\text{NaYF}_4:10\%$ Eu^{3+} nanoparticles.